

Annals of Nuclear Energy
An Uncertainty Quantification Method Relevant to Material Test Reactors
--Manuscript Draft--

Manuscript Number:	ANUCENE-D-21-00267
Article Type:	Full Length Article
Keywords:	uncertainty quantification; material test reactors; graphite irradiation; total Monte Carlo
Abstract:	Within material test reactor calculations, spectrum and reaction rate uncertainties are typically not quantified when performing as-run analyses to determine the neutron field experienced by the experiment. Methods to propagate uncertainties through high fidelity simulations are available when sufficient computational power is available. A tool is developed for sampling MCNP inputs from random distributions to determine output uncertainties based on those inputs. Another tool is developed to sample nuclear data cross-section in ACE format using multi-group nuclear data covariances. The Total Monte-Carlo Method and GRS are implemented and compared to one another as well as MCNP sensitivity and uncertainty calculations. The methods were applied to calculate uncertainties in spectrum and reaction rates for the Godiva sphere, UAM-pincell benchmark, and Advanced Test Reactor. The methods agree well, with GRS allowing for an order of magnitude speedup for reaction rate uncertainty calculations and several orders of magnitude for eigenvalue uncertainty calculations.

1
2
3
4
5
6
7
8
9
10
11
12

An Uncertainty Quantification Method Relevant to Material Test Reactors

13 Vishal Patel^{a,*}, Jorge Navarro^b, William Windes^c, Pavel Tsvetkov^d
14

15 ^a2356 W Commodore Way, Seattle, WA 98199
16 ^bP.O. Box 2008 Oak Ridge, TN 37831
17 ^c1955 N. Fremont Ave. Idaho Falls, ID 83415
18 ^d3127 TAMU, College Station, TX 77843-3127

21 22 Abstract

23
24 Within material test reactor calculations, energy dependent flux and reaction
25 rate uncertainties are typically not quantified when performing as-run analyses
26 to determine the neutron field experienced by the experiment. When high fidelity
27 Monte-Carlo codes are used in such analyses, straight forward methods
28 to calculate output uncertainties are not available, instead expert opinion is
29 used to postulate computational uncertainties. New methods to propagate un-
30 certainties through these high fidelity simulations are available when sufficient
31 computational power is available. A tool is developed for sampling any part of
32 an MCNP input from random distributions to determine output uncertainties
33 based on those inputs. Another tool is developed to sample nuclear data cross-
34 section in ACE format using multi-group nuclear data covariances. The Total
35 Monte-Carlo Method and **GRS** are implemented and compared to one another
36 as well as MCNP sensitivity and uncertainty calculations. The methods were
37 applied to the Godiva critical sphere k-eigenvalue, the UAM pin cell benchmark
38 energy dependent flux and reaction rates, and the Advanced Test Reactor en-
39 ergy dependent flux within an experimental location. The two methods agree
40 well, with GRS allowing for an order of magnitude speedup for reaction rate un-
41 certainty calculations and several orders of magnitude for eigenvalue uncertainty
42
43
44
45
46
47
48
49
50
51
52

53
54 *Corresponding author
55
56 URL: www.usnc-tech.com (Vishal Patel), www.ornl.gov (Jorge Navarro), www.inl.gov
(William Windes), <https://engineering.tamu.edu/nuclear/index.html> (Pavel Tsvetkov)

1
2
3
4
5
6
7
8
9 calculations.

10 *Keywords:* uncertainty quantification, material test reactors, nuclear data
11 uncertainties

15 1. Introduction

16 Material test research reactors focus on accelerated material degradation
17 experiments in radiation environments and isotope production. Many material
18 changes within the reactor are a function of the energy dependent neutron flu-
19 ence received over the experiment lifetime, and to correlate neutron damage
20 effects on materials, the fluence must be well known. The reactors have online
21 flux measurements and coolant temperature rise sensors to quantify the total
22 reactor power level. Many experiments are equipped with radiation flux wires
23 to quantify the fluence of neutrons over the total experiment lifetime. Neu-
24 tronic analysis is also performed after irradiations to predict the neutron flux
25 experienced by the experiment sample. These predicted fluxes are crucial to
26 the derived experiment data because the predicted fluxes are highly detailed
27 whereas the experimental data is quite sparse. Thus it is important to compute
28 the predicted flux well, and to include uncertainties in the results.

29 The results from online power measurements, counted radiation wires, and
30 computational analysis are combined to determine the actual neutron fluence
31 that the experiment received. The data de-convolution process takes into ac-
32 count uncertainties from all measurement sources to determine the fluence re-
33 ceived by an experiment, plus the uncertainty of the result. The computational
34 uncertainty often dominates the total uncertainty of energy dependent fluence
35 because only a few flux wire measurements are available to quantify the neu-
36 tron spectrum. However, uncertainties from the computational analysis are not
37 well determinable such that expert opinion is used for uncertainty instead of
38 model-based uncertainty. The main difficulties in determining these uncertain-
39 tities comes from tracking uncertain data inputs (fuel burnup, control positions,
40 changing power levels, . . . through computationally intensive Monte-Carlo (MC)

1
2
3
4
5
6
7
8
9 calculations. In order to better understand experiments, the computational un-
10 certainty must be quantified.
11

12 Models of material test reactors tend to include as much detail as possible
13 and thus rely upon Monte-Carlo codes where the details can be modeled. Un-
14 certainty quantification (UQ) and sensitivity analysis (SA) methods for Monte-
15 Carlo codes tend to concentrate on k-eigenvalue and not reaction rates. The
16 Monte-Carlo-N-Particle transport code [1] is used in many research facilities,
17 as such, this tool is selected to perform neutronics calculations. A literature
18 review was performed to find an efficient method to propagate uncertainties
19 with MCNP. A cross-section sampling and MCNP input file sampling method
20 was then implemented. MCNP parsers were created to efficiently apply the se-
21 lected UQ techniques. The UQ method was then compared to the UAM pincell
22 benchmark by means of k-eigenvalue uncertainty calculations.
23
24

25 **2. Background**
26
27

28 *2.1. Neutronic Uncertainty Quantification*
29

30 *2.1.1. Deterministic Methods*
31

32 The first developments of UQ/SA occurred with respect to the neutron trans-
33 port equation under the diffusion approximation [2], which was later generalized
34 under the Adjoint Sensitivity Analysis Procedure (ASAP) [3]. Within a multi-
35 group framework, UQ/SA has been performed and implemented in production
36 tools. Specifically, the adjoint multi-group transport equation can be solved
37 with small changes in the physics kernels in both deterministic and Monte-Carlo
38 solutions. For continuous energy adjoint calculations the situation is different.
39
40 Group to group scattering cross-sections cannot be easily inverted because cross-
41 sections are represented as relations and not discrete points. By representing
42 the scattering matrix as discrete points, the computer memory requirements for
43 calculations grows to unfeasible amounts. For continuous energy codes, other
44 methods have been developed to propagate uncertainties.
45
46
47
48
49
50
51
52
53
54
55
56
57
58
59
60
61
62
63
64
65

1
2
3
4
5
6
7
8
9 55 *2.1.2. Monte-Carlo Based Methods*

10
11 Effects of perturbations on a response can be directly calculated from for-
12 ward Monte-Carlo calculations, e.g., no need to run parametric studies for small
13 perturbations. In general, the perturbed parameters are nuclear data related
14 and the response function is the criticality eigenvalue. These calculations predict
15 sensitivity profiles and output uncertainties can be determined from multiplying
16 the magnitude of uncertainties with sensitivities.

17 The differential operator sampling (DOS) method [4] assumes the effect of
18 the perturbation being made (usually nuclear data) can be represented by a
19 Taylor series expansion around the mean value, generally using a 1st or 2nd
20 order expression. The derivative involved in the series expansion can be calcu-
21 lated using Monte-Carlo means. The original developments did not include all
22 the required steps to get generally correct answers. The fission source was not
23 perturbed during sampling such that a bias was introduced [5]. The method-
24 ology without the fission source perturbation will tend to disagree with similar
25 perturbation calculations [6].

26 The adjoint flux can in principle be calculated using Monte-Carlo methods,
27 though efficient methods to do so are difficult to implement for continuous *in* en-
28 ergy problems. In general to solve the problem would require an inverse random
29 walk from the end of the calculation to the beginning, e.g., a backwards calcula-
30 tion. Recently, the iterated fission probability (IFP) method [7] has been used to
31 determine the adjoint flux from forward *monte* calculations. This method relies
32 on the physical interpretation of the adjoint flux as an importance weighting[2];
33 it is the affect of a neutron introduced somewhere in phase space of a critical
34 system. This means during power source iterations, keeping track of what a
35 neutron produced in some iteration *i* does in a later iteration asymptotic gen-
36 eration *n* can allow for a creation of the adjoint flux. This adjoint can then
37 be used in typical deterministic manners using the sandwich rule to determine
38 sensitivities. Furthermore, it has been shown [8] that this method of adjoint
39 calculation is equivalent to the differential operator sampling method with fis-

1
2
3
4
5
6
7
8
9
10
11
12
13
14
15
16
17
18
19
20
21
22
23
24
25
26
27
28
29
30
31
32
33
34
35
36
37
38
39
40
41
42
43
44
45
46
47
48
49
50
51
52
53
54
55
56
57
58
59
60
61
62
63
64
65
85 sion source perturbations. A drawback of this method is that a large computer
memory is required due to storing of many histories as well as their original
birth conditions. The memory requirement is proportional to the number of
particles kept track of in each generation and the number of latent generations
used to establish an asymptotic case.

90 Contribution-Linked eigenvalue sensitivity/Uncertainty estimation via Track-
length importance CCharacterization (CLUTCH) [9] is a similar to the integrated
fission probability method was recently implemented in SCALE. This method
avoids some pitfalls of the IFP method in that computer memory requirements
do not scale directly with the number of particle histories. This is accomplished
95 by following particle histories directly from birth to death and computing rel-
evant MC integrals once a particle dies. The methodology agrees with well
multi-group MC methods as well as the IFP [9].

96 The DOS, IFP, and CLUTCH methods are good at S/U calculations for
system wide (integral quantities) such as k_{eff} , and kinetics parameters but has
100 difficulties determining specific tallies like dosimeter calculations because of the
large amount of memory required to track all neutrons through generations.
The CLUTCH method has the potential to reduce memory requirements and
perform sensitivity calculations though has not been completely implemented
in any production tool.

105 The Total Monte-Carlo (TMC) method, first introduced to propagate nu-
clear data uncertainty through reactor physics calculations [10] is a method to
propagate uncertainties with deterministic and MC methods. It is in essence
a general sampling method that uses a brute-force approach. Many random
110 inputs to a MC code are created, ran for a long time to get good MC statistics,
then uncertainties on outputs from input changes can be found by observing the
output distribution and subtracting MC uncertainties. It is an excellent method
to propagate input uncertainties through MC calculations, but takes a very long
time to perform, needing at least 500 calculations with random inputs, e.g., 500
times longer than a single run. This method is used in this work and will be
115 described in more detail in Sec. 3.1.

1
2
3
4
5
6
7
8
9 The GRS method [11] is similar to TMC where simulations are run many
10 times with inputs randomly selected and outputs stored for statistical analysis
11 to determine uncertainties. However, this method does not have the drawback
12 of needing to run each simulations for a long time. Rather, N simulations with
13 different inputs are run for a short time with a single random number seed,
14 then each N simulation is reran with a different random number seed (totaling
15 about twice the runtime of a single long calculation). The two different random
16 number seed simulations have identical MC (aleatoric) uncertainty distributions.
17 The covariance of the output sets is the epistemic uncertainty of the varying
18 inputs [11] because the MC uncertainty is almost eliminated (goes to zero as
19 MC sample batch sizes increases). This method is used in this work and will be
20 described in more detail in Sec. 3.2.

21
22
23 2.2. Nuclear Data Sampling

24
25 A main sources of uncertainty for transport and depletion calculations are
26 based on uncertainties of nuclear data. In general, nuclear data is created
27 from experimental means [12], however to resolve the quickly varying portions
28 of cross-sections as well as temperature dependence, evaluators create evalua-
29 tions [13]. Cross-sections can also be created from a theoretical basis and
30 corrected with experimental results [14]. Uncertainties in cross-sections are
31 complex because of correlations between different reaction channels as well as
32 variances in channels themselves. These uncertainties are stored in nuclear data
33 evaluations as covariance matrices. Recently, there has been an effort to per-
34 turb nuclear data directly through sampling. These created nuclear data are
35 then used in the transport calculation of choice to propagate the nuclear data
36 uncertainty. It should be noted that processing evaluating nuclear data files is
37 not a trivial process with many codes [15, 16, 17] dedicated to the task.

38
39 Perturbation theory offers similar calculations with multi-group nuclear data
40 and has been historically the tool of choice for sensitivity and uncertainty quan-
41 tification, for example SCALE’s TSUNAMI [18] uses this method. The nuclear
42 data sampling described is based on Monte-Carlo approaches, thus allowing the
43

1
2
3
4
5
6
7
8
9 data to be used with any transport approximation instead of just multi-group
10 calculations. An unfortunate aspect of the nuclear data sampling tools are
11 they are either proprietary or in-house implementations, thus not easily avail-
12 able. Open source tools [19] to manipulate nuclear data exist, however concise,
13 reliable APIs to use the methods developed are not yet available. The TENDL-
14 2012 [20] nuclear data library published many iterations of randomly created
15 data and is the largest source of openly available random nuclear data.
16
17
18
19

20 21 *2.2.1. Continuous Energy Covariance Based*

22
23 Evaluated nuclear data comes with multi-group covariance matrices to de-
24 scribe cross-section uncertainties. Tools have been developed to use these covari-
25 ances to sample nuclear data. Nuclear Data Uncertainty Analysis (NUDANA) [21]
26 and KIWI [22] are two such tools. A drawback of using nuclear data covariances
27 is that covariances are not available for all nuclide and are not all available for all
28 reaction channels. Nonetheless, the available covariances can be used to sample
29 nuclear data.
30
31
32

33 34 *2.2.2. Multi-Group Covariance Based*

35 Often reactor physics codes use the multi-group approximation to make
36 problems tractable. Continuous data can be collapsed into suitable energy bins
37 by various means to create multi-group nuclear data. Nuclear data covariances
38 can then be used to adjust the multi-group data after collapse. The Cross Sec-
39 tion Uncertainty and Sensitivity Analysis (XSUSA) [23] tool implements this
40 method of cross-section sampling. It's built to be create nuclear data with the
41 SCALE covariance matrices for use with the TSUNAMI sequence.
42
43
44
45
46
47

48 49 *2.2.3. Theoretical Model Based*

50 The TALYS Evaluated Nuclear Data Library (TENDL) [14] is a complete nu-
51 clear data library based on theoretical calculations along with specific evaluated
52 data. The use of theoretical calculations allows for evaluations of cross sections
53 that have not been measured and the creation of covariance matrices that have
54 not been measured. The library is created to agree with benchmarked data as
55
56
57
58
59
60
61
62
63
64
65

1
2
3
4
5
6
7
8
9
10
11
12
13
14
15
16
17
18
19
20
175 much as possible. It features many isotopes of interests and many, many more covariances than typical libraries that rely more on experimental data. Due to the computational nature of library creation, random nuclear data evaluations can be made using inputs to the theoretical model rather than relying on provided nuclear data covariances. The model inputs are varied until many sets
180 of cross sections are made that are not rejected (e.g., agree with experimental data).

21 2.2.4. ACE Data Based

22
23 A more direct method of sampling is to use vary the ACE (A Compact
24 ENDF) data format that MCNP and other transport codes use. ACE data
25
26 185 stores nuclear data in a point-wise manner such that linear interpolations can
27 be made between points to create ‘continuous’ data. The Nuclear data Un-
28 certainty Stochastic Sampling (NUSS) tool [24] directly perturbs the pointwise
29 data based on multi-group nuclear data covariances. This eliminates the need
30 33 to manipulate very complex ENDF data, but requires confidence in inputted co-
31 variance matrices. A comparison of NUSS and theoretical model based nuclear
32 35 data perturbations was performed previously [25]. The two methods agreed well
33 36 for benchmark criticality cases. However, there are cases where the theoretical
34 37 model produced nuclear data with a non-zero skewness, which are not repre-
35 38 sented in ENDF data. These skewed data leads to skewed uncertainties which
36 39 could be important in some safety calculations. The NUSS tool was also ex-
37 40 tended [26] with better statistical methods to perform global sensitivity analysis
38 41 based on the group-wise covariances and sampled made. The new method uses a
39 42 relatively complicated sampling scheme that assumes normal distributions. The
40 43 sampling method in this paper relies on ACE data with sampling philosophies
41 44 similar to NUSS.
42
43
44
45
46
47
48
49
50
51
52
53
54
55
56
57
58
59
60
61
62
63
64
65

1
2
3
4
5
6
7
8
9 **3. Uncertainty Quantification Methods**

10
11 *3.1. Total Monte-Carlo*

12
13 The Total Monte-Carlo method refers to a technique to randomly vary fundamental nuclear data parameters to generate many random nuclear data libraries
14 from theoretical models. These random data are used in many long running MC
15 calculations to determine the effects of nuclear data variations. The statistical
16 method to remove the MC statistics from output calculations can be described
17 by breaking up the observed uncertainty into Monte-Carlo and input uncertainties,
18
19
20
21
22
23

24
25
$$\sigma_{ob} \approx \bar{\sigma_s^2} + \sigma_i^2 \quad (1)$$

26
27
$$\bar{\sigma_s^2} = \frac{1}{N} \sum_{j=1}^N \sigma_{s,j}^2, \quad (2)$$

28 where σ indicates uncertainties, and the subscripts ob, s, i , indicate observed,
29 statistical, input uncertainties, and N is the total number of observations. If a
30 set of observations due to varying inputs can be made along with the associated
31 MC uncertainty, the input uncertainty can be determined using Eq. (1).

32 A large (500-1000) set of random inputs are generated to create a large
33 set of outputs. Within an MC calculation, each run should have sufficiently
34 low relative MC uncertainty (e.g., $\bar{\sigma_s} \approx 0.05$) such that the total uncertainty
35 observed from the large set of outputs is predominately from epistemic input
36 uncertainties. This method, though easy to implement for most code frameworks,
37 increases calculation time by 500-1000 times that of a single run. This
38 runtime is rather large for personal workstations but quite possible on modern
39 high performance computers where 1000s of processors are available for a single
40 user.

41 TMC has the added benefit of determining the full covariance of the re-
42 sponse [27]. This can be quite useful when performing spectrum adjustments.

43 Error estimates of the TMC results can be calculating using a bootstrap
44 method. The basic procedure is to take random samples of the random inputs

1
2
3
4
5
6
7
8
9
10
11
12
13
14
15
16
17
18
19
20
21
22
23
24
25
26
27
28
29
30
31
32
33
34
35
36
37
38
39
40
41
42
43
44
45
46
47
48
49
50
51
52
53
54
55
56
57
58
59
60
61
62
63
64
65

with replacement. The total number of random samples of the original samples to take should be equal to the original number of samples [28]. The `tmc` method is then applied to the new sampled inputs along with the corresponding outputs. This whole procedure is repeated many times to create a vector of uncertainty estimates. Confidence intervals can then be calculated by sorting the vector and calculating the lower and upper cutoffs based on a desired confidence interval.

3.2. GRS

The GRS method relies on the statistical distribution of MC outputs in order to determine input uncertainty. By taking two sets of random simulations, two distributions with the same uncertainties are found. The covariance of these distributions is the input uncertainty because statistical errors are the same in both sets and are removed by the covariance operation. In a mathematical sense, given a model, $Y = X(U)$, with input set U that is randomly varied, the average output μ , is,

$$\mu = \mathbf{E}[\mathbf{E}[Y|U]],$$

which given the results of iterated expectations (sometimes called law of total expectation),

$$\mu = \mathbf{E}[Y],$$

with variance, σ^2 as,

$$\sigma^2 = \text{Var}(\mathbf{E}[Y|U]).$$

The square-root of the variance gives the uncertainty of the inputs on the outputs. However, with a single MC run, a very large number of particles would need to be ran (like in TMC) to reduce MC statistics. However, when two sets of MC runs are made with two different random number seeds, two sets of outputs, Y, Y' are created that are conditionally independent and identically distributed, e.g., on average the outputs are the same but comparing individual

1
2
3
4
5
6
7
8
9 250 results will show differences ($\mu = \mathbf{E}[Y] = \mathbf{E}[Y']$). By using this fact and the
10 following form of the expectation of the two outputs multiplied, the variance of
11 the mean output can be related to the covariance between the two output sets.
12
13 The expectation of the two outputs multiplied is,

$$\begin{aligned} 15 \mathbf{E}[YY'] &= \mathbf{E}[\mathbf{E}[YY'|U]], \\ 16 &= \mathbf{E}[\mathbf{E}[Y|U] \cdot \mathbf{E}[Y'|U]], \\ 17 &= \mathbf{E}[\mathbf{E}[Y|U] \cdot \mathbf{E}[Y|U]], \\ 18 &= \mathbf{E}[\mathbf{E}[Y|U]^2]. \end{aligned} \quad (3)$$

24
25 Inserting Eq. (3) into the definition of covariance,
26
27
28
29
30
31
32
33
34
35
36
37
38
39
40
41
42
43
44
45
46
47
48
49
50
51
52
53
54
55
56
57
58
59
60
61
62
63
64
65
260 shows that the covariance between the two output sets is the variance of
the desired mean output given input uncertainties U . This formulation cancels
out (or averages) the MC uncertainties such that only the input uncertainties
remain. This method avoids Eq. (1) so criteria for $\bar{\sigma}_s^2$ are not required, though
MC uncertainties should be reasonably sized and enough particles ran to ensure
source convergence.

Covariance information cannot be generated from the GRS method because
the method targets the mean variance (diagonal of the covariance) and not
covariance information. A bootstrapping uncertainty estimator is also not valid
because the GRS method requires unique samples. However different estimators
could be used such as jack-knifing, but this is not explored in this work.

1
2
3
4
5
6
7
8
9 **4. Sampling Methods**

10
11 *4.1. Nuclear Data Sampling*

12
13 Randomly generated cross-section files available within TENDL are an excellent
14 resource, however random evaluations for all cross-sections are not available
15 and evaluated covariances are not used when generating the data. While the
16 latter is considered a positive feature of TENDL random data, it is not fully ac-
17 cepted that generated data from fundamental parameters is the correct method
18 of making nuclear data. The ability to generate random data with SCALE
19 based covariance data is a positive feature to overcome issues when data is not
20 available and to sample data based on evaluated distributions. A deficiency in
21 this method of sampling is that the covariance data must be available for the
22 reaction and nuclide of interest to actually sample data. Furthermore, sampling
23 from ENDF formatted covariances directly has a benefit of sampling from any
24 ENDF based data as well as from covariance data that has not yet made it to
25 official SCALE releases.
26
27
28
29
30
31
32
33

34 ASAPy¹ is a tool that was created in this work to perform data sampling
35 from ACE files using SCALE covariance data or ENDF data via NJOY to
36 address the above issues. This tool is similar to the NUSS tool described in
37 Sec. 2.2.4, except it uses the newest SCALE covariance data or newest ENDF
38 data, written in python, and available for use. It also features the ability to
39 use any group structure and/or any user flux weighting functions for covariance
40 collapsing from ENDF sources. The sampling procedures also uses lognormal
41 sampling along with the ability to use any sampling function as long as the
42 percent point function is available.
43
44
45
46
47
48

49 *4.2. ACE Data Manipulations*

50 The A Compact ENDF file (ACE) format is used for nuclear data within
51 MCNP and other Monte-Carlo codes. It contains all relevant data from ENDF

52
53
54
55 ¹<https://github.com/veeshy/ASAPy/releases/tag/v1.0>

1
2
3
4
5
6
7
8
9 files, support random access of data, and specifies all cross-sections on the same
10 unionized energy grid. The ACE data is a formatted data file and readers are
11 available, though writers tend to only translate ENDF data to ACE, with no
12 general method to manipulate the ACE data directly. The ACE data reader
13 within OpenMC [29] was used to read in ACE files. A writer was created based
14 on the structure of ACE files. All data is represented in contiguous arrays, so
15 that if the original data is known (from reading the ACE data), that data can
16 be searched for within the ACE file and replaced with new values as long as
17 the exact same energy grid is specified. This method of adjusting ACE data is
18 implemented in ASAPy. A few nuances when dealing with different data will
19 be discussed.

20
21
22
23
24
25
26 ***Cross-Section Perturbation:*** Nuclear data sampling occurs using multi-
27 group methods while ACE data is stored in a continuous format. Perturbation
28 factors are generated based on taking a ratio of sampled cross-sections and
29 multi-group average cross-sections. These perturbation factors are then ap-
30 plied to the continuous cross-sections by mapping the multi-group structure
31 on the continuous structure. This method can cause difficulties in sampling
32 data when a group boundary happens to occur in a region where the flux or
33 variance changes rapidly. This usually manifests itself in ill-formed covariance
34 information.

35
36
37
38
39
40 ***ENDF Sum Rules:*** Many ENDF reactions are subsets of other reactions,
41 so when one cross-section is sampled, others might need to be adjusted for
42 consistency. This is performed within ASAPy by keeping track of all MTs
43 adjusted and comparing against sum rules. Table 1 shows the relevant sum
44 rules from the ENDF manual [13].

45
46
47
48 ***$\bar{\nu}$ Data:*** ENDF data allows for inclusion of total, average number delayed,
49 and prompt fission neutrons. MCNP only uses the total values within ACE
50 files, so only these are modified.

51
52
53 ***Fission χ Spectrum:*** The distribution of energy of neutrons born from
54 fission depends on the incident neutron energy. As such, ACE data file stores
55 several tables for a few incident neutron energies. ENDF covariance data does
56

1
2
3
4
5
6
7
8
9
10
11
12
13
14
15
16
17
18
19
20
21
22
23
24
25
26
27
28
29
30
31
32
33
34
35
36
37
38
39
40
41
42
43
44
45
46
47
48
49
50
51
52
53
54
55
56
57
58
59
60
61
62
63
64
65

not have covariance data for each incident neutron so the covariance data within
325 the ENDF file is applied to all incident neutron energy distributions. The dis-
tributions are also stored as probability and cumulative distribution functions
(PDF and CDF). To sample these, the PDF is perturbed then the CDF is
adjusted based on the PDF perturbations then the CDF is re-normalized by
adding up the original PDF and perturbation factors to ensure the CDF sums
330 to 1.

21 4.3. Covariance Data

22
23 The most comprehensive resource for covariance data is distributed within
24 SCALE 6.2 [18]. It combines covariance data from several nuclear data sources
25 and experiments. The SCALE based data was generated using a typical LWR
26 flux that include a thermal, epi-thermal, and fast region. A fine 252-group
27 and coarse 56-group structure is available within SCALE. An older 44-group
28 structure exists but contains old data that is not recommended for use. The
29 covariance data can be converted from the internal SCALE binary format to a
30 ASCII format using the SCALE tool AmpxCOVConverter. The resulting data
31 335 file contains data for material numbers and their relevant reactions correlated
32 with one another. The standard deviations of the specified reactions are given
33 in the relevant group structure followed by the actual correlation matrix. A
34 covariance parser was created within ASAPy to convert the ASCII file to a
35 340 more general HDF5 store with a hierarchy based on: '/mat1/mt1/mat2/mt2'
36 corresponding to data correlating mat1 MT1 with mat 2 MT2. Often mat 1
37 and mat 2 are the same, and MT1 and MT2 are the same, specifying self-
38 correlation. Any group structure can be accommodated by the parser such that
39 new evaluations can be easily used within ASAPy.

40
41 Covariance data also exists in ENDF files and these covariances can be used
42 350 to create any group structure as well as use any weighting flux to create co-
43 variance matrices to sample with. ENDF data can be parsed with NJOY [15]
44 to generate covariance data. ASAPy implements NJOY input writers along
45 with ENDF readers to minimize the amount of user input to generate covari-
46
47
48
49
50
51
52
53
54
55
56
57
58
59
60
61
62
63
64
65

1
2
3
4
5
6
7
8
9
10
11
12
13
14
15
16
17
18
19
20
21
22
23
24
25
26
27
28
29
30
31
32
33
34
35
36
37
38
39
40
41
42
43
44
45
46
47
48
49
50
51
52
53
54
55
56
57
58
59
60
61
62
63
64
65
ance data. The minimum input is a path to an ENDF file and the reaction
355 MT numbers to generate covariance data for. A BOXER format reader was
also generated in order to read the BOXER formatted covariance files into the
previously described HDF5 format.

The covariance data comes in multi-group format which must be mapped to
relevant continuous energy bins in ACE data. After sampling data within the
360 multi-group structure, the data is divided by the multi-group mean cross-section
to calculate a relative cross-section. These cross-sections are mapped onto the
continuous energy group bins then multiplied by the ACE data to generate a
sample of data. Two assumptions made are that the group-mean values within
the data are very similar to the mean values within the ACE data and that the
365 data within an energy bin are fully-correlated with one another.

No data is shipped with ASAPy, ENDF data is freely available and SCALE
data is available with appropriate licenses.

32 4.4. Nuclear Data Sampling Techniques

A slight deficiency in the ENDF format is the inability for evaluators to
370 convey what type of distribution covariance data should take. Often physical
375 parameters like cross-sections cannot take negative values, but assuming
normal distributions are assigned to reported covariances, negative values are
possible. An approach often taken is to discard negative data, biasing the sam-
pling scheme. Another method is to assume the distributions are log-normal,
375 which always has positive values. However, without knowing what distributions
380 the covariance data were specified for, errors can occur when large relative er-
rors are present with strong negative correlations [30] due to not transforming
the normal-cov to lognormal-cov. In this work, ENDF covariance data is trans-
formed to log-normal covariance data then log-normal sampling is performed
ensuring no negative samples are taken.

Nuclear data has strong correlations between energy groups so when sam-
pling data, the full covariance of the data must be taken into account. Multivariate-
normal distributions allow for sampling of such data. Given a desired covariance

matrix, C , that is semi-positive definite, and mean values, μ , a multi-variate sample, X_i can be generated as follows. First draw uncorrelated values from the mean using a standard-normal distribution, \mathcal{N} and place the means in a diagonal matrix,

$$x_i = \mathcal{N}[\mu = 0, \sigma = 1],$$

then perform a singular value decomposition of the covariance,

$$C = USV, \quad (4)$$

where U and V are orthogonal matrices, and S is a diagonal matrix containing the singular values of C . A sample can then be drawn as

$$X_i = \mu + x_i S^{0.5} v$$

This method is implemented in Scipy [31] within ‘np.random.multivariate_normal’. One may also use eigen or Cholesky decomposition instead of singular value decomposition with similar results.

ENDF based nuclear data sometimes is published with non-semi-positive-definite covariances. In this case the correlation data R must be manipulated to draw samples. An eigen-decomposition of the correlation matrix is made,

$$R = Q\Lambda Q^{-1},$$

where Q contains the eigenvectors of R , and Λ contains the eigenvalues on the diagonal. The negative eigenvalues are set to a small positive number (1e-8) to form $\tilde{\Lambda}$ then the original eigenvectors are multiplied back in to form an adjusted correlation matrix, \tilde{R} ,

$$\tilde{R} = Q\tilde{\Lambda}Q^{-1}.$$

The correlation matrix is used due to smaller spreads in eigenvalues, however often the small eigenvalues imposed on the matrix cause numerical difficulties when converting the correlation matrix to a covariance matrix so the above procedure may need to be repeated on the converted covariance matrix.

A second method based on a partial Cholesky decomposition [32] that generates a positive semi-definite matrix that equals the original matrix minus an

MT	Description	MTs in Sum
1	Incident Neutron Total cross	2, 4, 5, 11, 16-18, 22-26, 28-37, 41-42, 44-45, 102-117
4	Total of neutron levels	50-91
18	Total fission	19-21, 38
103	Total of proton levels	600-649
104	Total of deuteron levels	650-699
105	Total of triton levels	700-749
106	Total of ^3He levels	750-799
107	Total of alpha levels	800-849

Table 1: ENDF Sum Rules

³⁹⁰ error term was also implemented for correcting non semi-positive definite matrices.

³⁹⁵ A non-semi positive definite correlation example is the correlation matrix for (n, γ) cross-section of ^{184}W within ENDFB/VIII. The eigen-decomposition and partial Cholesky algorithms were applied to generate 500 samples and the correlation matrices are shown in Fig. 1, where it can be seen that both algorithms perform well compared to the original correlation matrix.

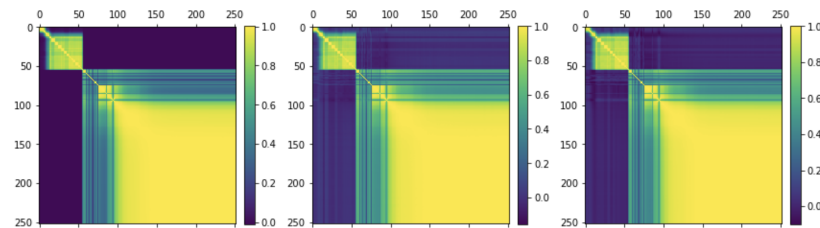


Figure 1: Correlation matrices from (left) the evaluated data file (middle) eigen-decomposition sampling (right) partial Cholesky decomposition sampling

1
2
3
4
5
6
7
8
9
10
11
12
13
14
15
16
17
18
19
20
21
22
23
24
25
26
27
28
29
30
31
32
33
34
35
36
37
38
39
40
41
42
43
44
45
46
47
48
49
50
51
52
53
54
55
56
57
58
59
60
61
62
63
64
65

4.5. MCNP Input Sampling

mcACE is a tool developed to perform UQ using MC methods. It is used to manipulate MCNP input files to create random perturbations based on changing any line given variables to change and distributions to sample from. It also handles data post-processing, data transfer, MCNP/ORIGEN coupling, and performs statistics on relevant results. ORIGEN coupling is not discussed in this paper but it is available in the code to help propagate uncertainties through time. The typical flow of mcACE is shown in Fig. 2.

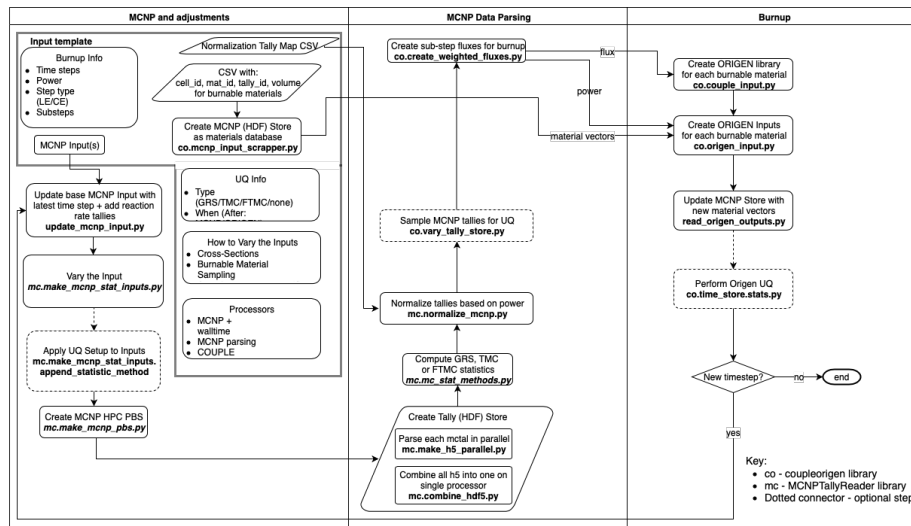


Figure 2: mcACE Flow Diagram

405 The goal of mcACE was to apply to many reactor designs rather than only
410 work with a single reactor. This goal necessitated writing a program that could
understand MCNP syntax. Particularly, MCNP cell lines can be parsed for cell
numbers, material numbers, densities, and volumes; MCNP problem lines can
be parsed for material numbers and materials. More subtle MCNP features
are also handled such as MCNP single line comments (C comment), end of line
comments (valid line \$ comment), and both types of continuation lines (lines
starting with 5 spaces and lines following a &). This allows for reading as well
as writing back MCNP files that can be ran with MCNP directly. The whole

1
2
3
4
5
6
7
8
9 input file is parsed into a python class that allows access to the MCNP title,
10 415 cell, surface, and problem blocks. Find and replace functions help sampling
11 procedures vary inputs.
12
13

14 Any parameter in the MCNP input can be sampled using the mcACE in-
15 put. This is similar to MCNP-PSTUDY [33], however more general samplers
16 are available. Given the original line and a properly formatted version of that
17 420 line, sampling can be performed. An example to vary density is shown in Fig. 1,
18 where the first line is the original MCNP line in pseudo-code format, and the
19 second line is the original line with the ‘density’ number replaced with a python
20 string formatter with index 0. The index 0 corresponds to the position in the
21 ‘sampling_scheme’ list. The ‘sampling_scheme’ allows for many sampling func-
22 tions like uniform, normal, latin-normal, repeating the last sampled value, giv-
23 425 ing an exact value for a simple find/replace, or a user generated math function.
24 This interface provides good flexibility to sample MCNP files. The mcACE in-
25 put allows for repeated sampling blocks so sets of parameters can be varied as
26 needed.
27
28
29
30
31
32
33
34
35
36
37
38
39
40
41
42
43
44
45
46
47
48
49
50
51
52
53
54
55
56
57
58
59
60
61
62
63
64
65

Listing 1: Sample mcACE MCNP Line Sampling SNippet

```
mcnp_lines=cellnum matnum density surf cards imp:n=1,  
lines_to_vary_with=cellnum matnum {0:.6f} surf cards imp:n=1,  
sampling_scheme=latin ,  
sampling_values=0.1 0.05 ,
```

430 4.6. MCNP Tally Reader

48 MCNP prints relevant outputs to ‘.o’ files, and optionally ‘.mctal’ files. The
49 ‘.o’ files contain a wealth of information, particularly about statistics and prob-
50 lem run information as well as relevant outputs like tallies and eigenvalue. The
51 ‘.mctal’ files contain a subset of the information in the ‘.o’ files but the infor-
52 435 mation is very structured, allowing for efficient readers to be created. mcACE
53 56 implements an ‘.mctal’ reader to read eigenvalues, problem information, and
54
55
56
57
58
59
60
61
62
63
64
65

1
2
3
4
5
6
7
8
9 most tallies (i.e., F#:particle, FC, E, T, C, FM, DE/DF, and SD), missing is a
10 mesh-tally reader though one could be added. MCNP ‘.o’ files can also be read
11 for information that is not present in a ‘.mctal’ file such as kinetics parameters
12 and sensitivity coefficients.
13
14 440

15
16 4.7. *mcACE Storage*
17

18 The UQ process implemented generates a large amount of output depending
19 on the relevant output parameters. In a typical run with 500 MCNP in
20 eigenvalue mode, 5 tallies with 100 energy bins would result in 2.5e5 outputs to
21 track. In a burnup calculation that uses a 238-group structure and 100 unique
22 materials, a minimum of 11.9e6 outputs must be tracked. Storing this data in
23 typical text files or csv’s is not efficient and error prone. mcACE opts to use
24 the HDF5 storage format along with Pandas [34] dataframes to store data as
25 tables in HDF5 format. After relevant outputs are parsed for each MCNP run,
26 all of the similar results are combined into a dataframe with multiple index as
27 tally info as needed and a run number index, with columns as energy bins or
28 other specific names such as ‘keff’. This format also makes it easier to perform
29 statistics on the outputs.
30
31
32
33
34
35
36
37
38
39
40
41 450

5. Verification and Application

42 5.0.1. *Godiva Eigenvalue*
43
44
45
46
47
48
49
50
51
52
53
54
55
56
57
58
59
60
61
62
63
64
65

460 The Godiva core is a well known benchmark model / experimental validation
461 core. It is a bare spherical mass of HEU that has a well quantified uranium mate-
462 rial vector and critical dimensions. It’s also a simple reactor core to analyze due
463 to it’s fast spectrum. The MCNP-IFP method was used to calculate sensitivi-
464 ties for several reaction MTs. Covariances were provided by ASAPy to calculate
465 the total uncertainty on eigenvalue from reaction rates via the sandwich rule.
466 The mcACE UQ process using TMC and ASAPy generated cross-sections was
467 performed using 1000 runs. Table 2 shows good agreement for all studied re-
468 action MTs, all values agree within uncertainty. MCNP-IFP uncertainty was
469
470

Correlation	Reaction	Unc. (pcm)	95% σ	MCNP-IFP
Uncorrelated	(n, γ)	479.4	13.3	482.3
	(n,f) + (n, γ)	493.5	13.3	-
	(n,f)	121.2	3.3	119.8
	$\bar{\nu}$	221.1	5.5	218.5
	Fission χ	167.4	5.0	169.3
Correlated	(n, γ)	838.8	24.4	848.9
	(n,f) + (n, γ)	883.3	25.1	-
	(n,f)	269.5	6.8	269.4
	$\bar{\nu}$	546.0	13.9	544.1
	Fission χ	269.0	12.7	276.2

Table 2: Comparing Godiva Uncertainties using ASAPy to MCNP-IFP

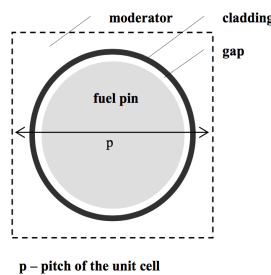
not propagated. This result shows that the TMC method agrees well with the IFP theory in terms of eigenvalue uncertainties. This indirectly shows the GRS method also agrees well with IFP theory in that it agrees well with TMC calculations, which will be shown in Sec. 5.0.2. Reaction rate uncertainties could not currently be calculated within MCNP for further verifications.

5.0.2. UAM Pincell Flux and Reaction Rates

To verify the GRS implementation the TMC (Total Monte-Carlo) method is used as the ‘true’ result. Furthermore, convergence studies are performed to determine how many runs are needed for GRS cases. The relative errors reported are the uncertainties in the output quantities from input uncertainty, and not the typical MCNP related statistical error. The relative errors of each value are compared by plotting the relative error of the GRS method to the TMC method. If the two methods agree, a point will be on the $y=x$ line.

The UAM Pincell Benchmark [35] at hot-zero power was modeled according to the specifications in Fig. 3. The TMC cases were ran with 7500 particles

480 / cycle for 15000 active cycles, the GRS cases used 40 cycles (187.5 times less total particles ran because GRS requires twice as many model runs). In Fig. 4 it can be seen that in general, GRS agrees well with TMC.



Parameter	Value
Unit cell pitch, [mm]	18.75
Fuel pellet diameter, [mm]	12.1158
Fuel pellet material	UO_2
Fuel density, [g/cm ³]	10.42
Fuel enrichment, [w/o]	2.93
Cladding outside diameter, [mm]	14.3002
Cladding thickness, [mm]	0.9398
Cladding material	Zircaloy-2
Cladding density, [g/cm ³]	6.55
Gap material	He
Moderator material	H ₂ O

Parameter / Reactor condition	HZP	HFP
Fuel temperature, [K]	552.833	900
Cladding temperature, [K]	552.833	600
Moderator (coolant) temperature, [K]	552.833	557
Moderator (coolant) density, [kg/m ³]	753.978	460.72
Reactor power ,[MWt]	3.293	3 293
Void fraction (%)	-	40

Figure 3: UAM PinCell Dimensions [35]

5.1. Practical Example with Advanced Test Reactor

The Advanced Test Reactor (ATR) [36] is a high powered, high flux material test reactor used for isotope production, fuel qualification, material irradiations, and other experiments. Often the irradiation history of an experiment can be determined through purely experimental means like determining the fission rate of a fueled sample via microscopy or calculating activity via radiation detectors. Other times flux wires must be used along with computer models to determine the irradiation history. When computer models are needed, an estimate of the uncertainty of the relevant computation is important. To show the usefulness of TMC and GRS methods on a real world model, the uncertainty of the flux in an experiment within the ATR was calculated.

The energy dependent flux within graphite shown is very important in determining spectral adjustments based on experiment flux wires. Each model

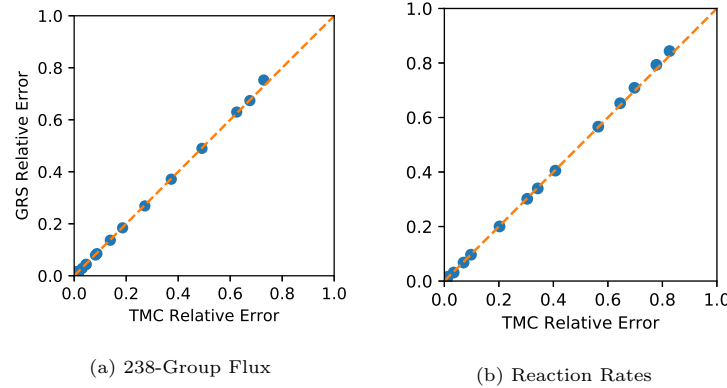


Figure 4: TMC and GRS Relative Uncertainties

ran has a unique U-235 data library created from TENDL-12 ENDF files [20]. The predicted GRS relative errors (shown in Fig. 5) for the 148.75x case shows reasonable agreement (mosth within 20%) with the TMC values. Grouping of TMC values near the y-axis (x=0) that TMC failed to predict the input errors because of relatively large MC standard deviations or large MC variance to observed variance ratios in the calculated values. This shows that the GRS method is able to predict relative output uncertainties where the TMC method fails. This does not show that the GRS method predicts a similar value to TMC in those cases if TMC were able to predict a value, though it's a reasonable conclusion because the two agree well when TMC is applicable.

The speedup for the GRS method for energy dependent flux is not as great as global values like eigenvalue. Excellent agreement between the TMC and the GRS cases occur when 12.9x less particles are used in GRS than TMC. The 37.19x less particle case has slightly more spread in results but all values where comparable agree with 20%.

6. Conclusions

A process was developed to quantify uncertainty of any output with an established Monte-Carlo neutronic code (MCNP) without any source code modification and built into a new code called mcACE. A review of relevant method

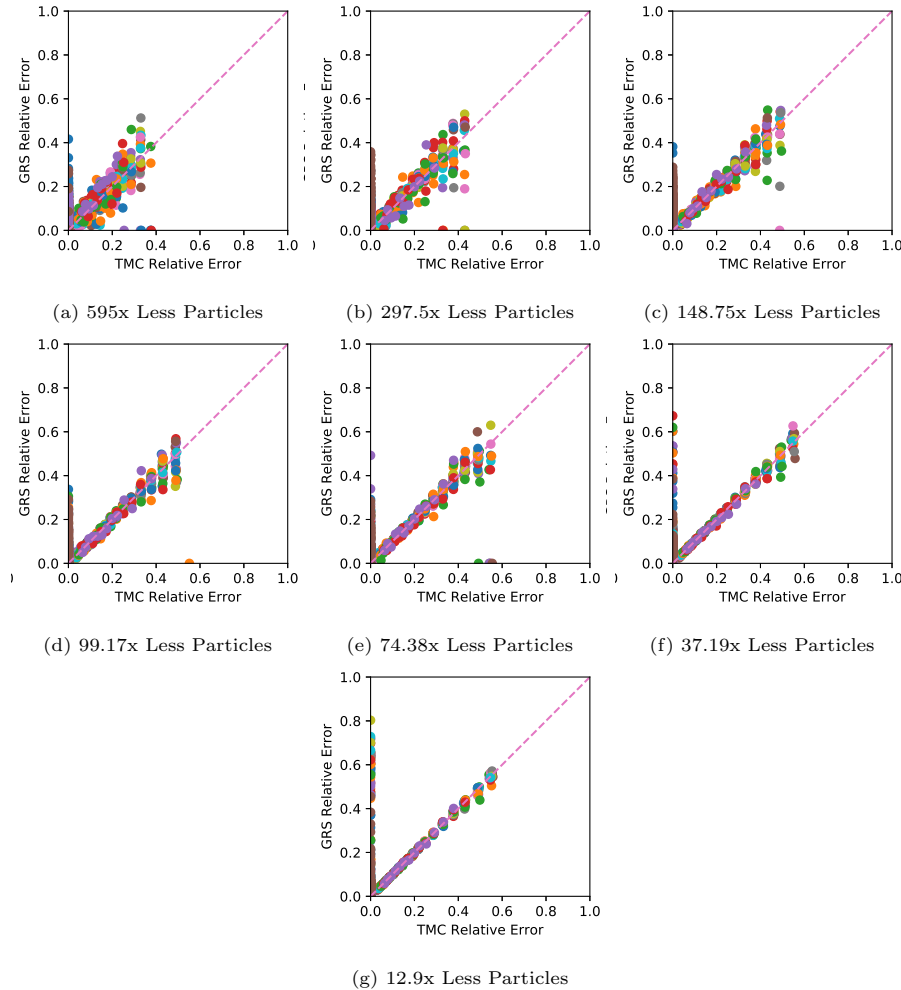


Figure 5: Various Runtimes Predicting Graphite Flux Using GRS

1
2
3
4
5
6
7
8
9 515 was performed and a combination of sampling techniques and statistical meth-
10 ods were identified to perform uncertainty quantification of relevant outputs for
11 reactor calculations. Comparisons of the selected statistical methods, GRS and
12 TMC were made to confirm their ability to predict similar outputs. GRS showed
13 an decrease of at least 10x computational time relative to TMC when calculating
14 uncertainties of fine-group fluxes in small regions of a reactor model. For larger
15 regions or more global values, 100x or more speedup is possible. The TMC
16 method was shown to also compare well with traditional sensitivity methods
17 when applied to k-eigenvalue calculations.
18
19

20 ASAPy was created to sample ACE data based on ENDF and SCALE co-
21 variances using normal and log-normal distributions. ASAPy can generate co-
22 variance from ENDF data for any group structure and any spectrum weight.
23 Data is generated as ACE files and methods were developed to update MCNP
24 data tables so that the ACE Files can be used. Generated cross-sections were
25 verified to produce similar uncertainties in the Godiva reactor as adjoint based
26 methods.
27
28

29 Finally the TMC and GRS methods were applied to a real-world model of
30 the Advanced Test Reactor to successfully calculate an energy dependent flux
31 within an experimental location. The two methods agreed well again, with the
32 GRS method being at least 10x faster.
33

34 535 Future work should include further code-to-code verifications and new
35 nuclear data sampling treatments. In particular, comparisons of reaction rate
36 uncertainties from other codes and energy dependent flux uncertainties are of
37 interest. Sampling methods with built-in sensitivity calculation methods [26]
38 could also be used to add calculations of sensitivity profiles. Sampling methods
39 with decreased sampling requirements [37] could also be implemented.
40
41

52 References

53 [1] J. T. Goorley, M. R. James, T. E. Booth, F. B. Brown, J. S. Bull, L. J.
54 Cox, J. W. J. Durkee, J. S. Elson, M. L. Fensin, R. A. I. Forster, J. S.
55
56
57
58

1
2
3
4
5
6
7
8
9
10
11
12
13
14
15
16
17
18
19
20
21
22
23
24
25
26
27
28
29
30
31
32
33
34
35
36
37
38
39
40
41
42
43
44
45
46
47
48
49
50
51
52
53
54
55
56
57
58
59
60
61
62
63
64
65

Hendricks, H. G. I. Hughes, R. C. Johns, B. C. Kiedrowski, R. L. Martz, S. G. Mashnik, G. W. McKinney, D. B. Pelowitz, R. E. Prael, J. E. Sweezy, L. S. Waters, T. Wilcox, A. J. Zukaitis, Initial MCNP6 Release Overview - MCNP6 version 1.0, Los Alamos National Laboratory (April 2013).

- [2] E. P. Wigner, Effect of small perturbations on pile period, in: Nuclear Energy, Springer, 1992, pp. 540–552.
- [3] D. Cacuci, Sensitivity & Uncertainty Analysis, Volume 1: Theory, CRC Press, 2003.
URL <https://books.google.com/books?id=6HzSuyJ15AoC>
- [4] H. Rief, Generalized monte carlo perturbation algorithms for correlated sampling and a second-order taylor series approach, *Annals of Nuclear Energy* 11 (9) (1984) 455 – 476. doi:[http://dx.doi.org/10.1016/0306-4549\(84\)90064-1](http://dx.doi.org/10.1016/0306-4549(84)90064-1).
URL <http://www.sciencedirect.com/science/article/pii/0306454984900641>
- [5] Y. NAGAYA, T. MORI, Impact of perturbed fission source on the effective multiplication factor in monte carlo perturbation calculations, *Journal of Nuclear Science and Technology* 42 (5) (2005) 428–441. doi:[10.1080/18811248.2005.9726411](https://doi.org/10.1080/18811248.2005.9726411).
URL <http://www.tandfonline.com/doi/abs/10.1080/18811248.2005.9726411>
- [6] Comparison of the Monte Carlo adjoint-weighted and differential operator perturbation methods.
- [7] B. C. Kiedrowski, F. B. Brown, P. Wilson, Calculating kinetics parameters and reactivity changes with continuous-energy monte carlo, Tech. rep., Los Alamos National Laboratory (LANL) (2009).
- [8] H. J. SHIM, C. H. KIM, Adjoint sensitivity and uncertainty analyses in monte carlo forward calculations, *Journal of Nuclear Science and Technol-*

ogy 48 (12) (2011) 1453–1461. doi:10.1080/18811248.2011.9711838.

URL <http://www.tandfonline.com/doi/abs/10.1080/18811248.2011.9711838>

C. M. Perfetti, B. T. Rearden, W. R. Martin, Scale continuous-energy eigenvalue sensitivity coefficient calculations, Nuclear Science and Engineering 182 (3) (2016) 332–353.

A. Koning, D. Rochman, Towards sustainable nuclear energy: Putting nuclear physics to work, Annals of Nuclear Energy 35 (11) (2008) 2024 – 2030. doi:<http://dx.doi.org/10.1016/j.anucene.2008.06.004>.

URL <http://www.sciencedirect.com/science/article/pii/S0306454908001813>

W. Zwermann, B. Krzykacz-Hausmann, L. Gallner, M. Klein, A. Pautz, K. Velkov, Aleatoric and epistemic uncertainties in sampling based nuclear data uncertainty and sensitivity analyses, Tech. rep., American Nuclear Society, Inc., 555 N. Kensington Avenue, La Grange Park, Illinois 60526 (United States) (2012).

N. Otuka, et al., Towards a more complete and accurate experimental nuclear reaction data library (exfor): International collaboration between nuclear reaction data centres (nrdc), Nuclear Data Sheets 120 (2014) 272 – 276. doi:<http://dx.doi.org/10.1016/j.nds.2014.07.065>.

URL www.sciencedirect.com/science/article/pii/S0090375214005171

M. Herman, A. Trkov, Endf-6 formats manual, National Nuclear Data Centre, BNL, Upton, New York.

A. J. Koning, D. Rochman, Modern nuclear data evaluation with the talys code system, Nuclear data sheets 113 (12) (2012) 2841–2934.

D. Muir, R. Boicourt, A. Kahler, The njoy nuclear data processing system, version 2012, Tech. rep., LA-UR-12-27079 (2012).

1
2
3
4
5
6
7
8
9
10
11
12
13
14
15
16
17
18
19
20
21
22
23
24
25
26
27
28
29
30
31
32
33
34
35
36
37
38
39
40
41
42
43
44
45
46
47
48
49
50
51
52
53
54
55
56
57
58
59
60
61
62
63
64
65

600 [16] D. E. Cullen, Prepro 2015 2015 endf/b pre-processing codes, Tech. rep.,
IAEA-NDS-39 (2015).

605 [17] D. Wiarda, M. L. Williams, C. Celik, M. E. Dunn, Ampx: A modern cross
section processing system for generating nuclear data libraries, Tech. rep.,
Oak Ridge National Laboratory (2015).

610 URL <http://www.osti.gov/scitech/servlets/purl/1286858>

615 [18] B. Rearden, M. Jessee, Scale code system, Tech. Rep. ORNL/TM-2005/39,
Oak Ridge National Laboratory (2016).

620 [19] C. Mattoon, B. Beck, N. Patel, N. Summers, G. Hedstrom, D. Brown,
Generalized nuclear data: a new structure (with supporting infrastructure)
for handling nuclear data, Nuclear Data Sheets 113 (12) (2012) 3145–3171.

625 [20] S. C. van der Marck, A. J. Koning, D. A. Rochman, Benchmarking tendl-
2012, Nuclear Data Sheets 118 (2014) 446–449.

630 [21] O. Buss, A. Hoefer, J.-C. Neuber, Nuduna: “nuclear data uncertainty anal-
ysis”, in: Meeting on uncertainty propagations in the nuclear fuel cycle
Uppsala University, 2013.

635 [22] J. Pruet, Kiwi: An evaluated library of uncertainties in nuclear data and
package for nuclear sensitivity studies, Tech. rep., Lawrence Livermore Na-
tional Laboratory (LLNL), Livermore, CA (2007).

640 [23] W. ZWERMANN, A. AURES, L. GALLNER, V. HANNSTEIN,
B. KRZYKACZ-HAUSMANN, K. VELKOV, J. MARTINEZ, Nuclear
data uncertainty and sensitivity analysis with xsusa for fuel assembly
depletion calculations, Nuclear Engineering and Technology 46 (3) (2014)
343 – 352. doi:<http://dx.doi.org/10.5516/NET.01.2014.711>.

645 URL <http://www.sciencedirect.com/science/article/pii/S1738573315301297>

650 [24] T. Zhu, Sampling-based nuclear data uncertainty quantification for contin-
uous energy monte carlo codes, Ph.D. thesis, EPFL (2015).

1
2
3
4
5
6
7
8
9 [25] D. Rochman, A. Vasiliev, H. Ferroukhi, T. Zhu, S. van der Marck, A. J.
10 Koning, Nuclear data uncertainty for criticality-safety: Monte carlo vs.
11
12 linear perturbation, *Annals of Nuclear Energy* 92 (2016) 150–160.
13
14 [26] T. Zhu, A. Vasiliev, H. Ferroukhi, A. Pautz, S. Tarantola, Nuss-rf: stochastic
15 sampling-based tool for nuclear data sensitivity and uncertainty quantification,
16 *Journal of Nuclear Science and Technology* 52 (7-8) (2015)
17 1000–1007. [arXiv:https://doi.org/10.1080/00223131.2015.1040864](https://doi.org/10.1080/00223131.2015.1040864),
18
19 doi:10.1080/00223131.2015.1040864.
20
21 URL <https://doi.org/10.1080/00223131.2015.1040864>
22
23
24 [27] N. Asquith, S. van der Marck, Using total monte carlo to calculate the
25 full covariance matrix of a neutron spectrum, in: *Reactor Dosimetry: 16th*
26 *International Symposium*, ASTM International, 2018.
27
28
29
30 [28] M. Kuhn, K. Johnson, *Applied predictive modeling*, Vol. 26, Springer, 2013.
31
32 [29] P. K. Romano, N. E. Horelik, B. R. Herman, A. G. Nelson, B. Forget, K. Smith, Openmc: A state-of-the-art monte carlo code for
33 research and development, *Annals of Nuclear Energy* 82 (2015) 90
34 – 97, joint International Conference on Supercomputing in Nuclear
35 Applications and Monte Carlo 2013, SNA + MC 2013. Pluri- and
36 Trans-disciplinarity, Towards New Modeling and Numerical Simulation
37 Paradigms. doi:<https://doi.org/10.1016/j.anucene.2014.07.048>.
38
39 URL <http://www.sciencedirect.com/science/article/pii/S030645491400379X>
40
41
42
43
44
45
46
47 [30] G. Žerovnik, A. Trkov, D. L. Smith, R. Capote, Transformation of corre-
48 lation coefficients between normal and lognormal distribution and implica-
49 tions for nuclear applications, *Nuclear Instruments and Methods in Physics*
50 *Research Section A: Accelerators, Spectrometers, Detectors and Associated*
51 *Equipment* 727 (2013) 33–39.
52
53
54
55
56 [31] E. Jones, T. Oliphant, P. Peterson, et al., SciPy: Open source scientific
57
58
59
60
61
62
63
64
65

1
2
3
4
5
6
7
8
9 tools for Python, [Online] (2001–).

10 URL <http://www.scipy.org/>

11
12 [32] J. Nocedal, S. J. Wright (Eds.), Numerical Optimization, Springer-Verlag,
13 1999. doi:10.1007/b98874.

14
15
16 URL <https://doi.org/10.1007/b98874>

17
18 [33] F. B. Brown, J. E. Sweezy, R. Hayes, Monte carlo parameter studies and
19 uncertainty analyses with mcnp5, in: PHYSOR-2004, American Nuclear
20 Society Reactor Physics Topical Meeting, 2004.

21
22 [34] T. pandas development team, pandas-dev/pandas: Pandas (Feb. 2020).

23
24 URL <https://doi.org/10.5281/zenodo.3509134>

25
26 [35] K. Ivanov, M. Avramova, S. Kamerow, I. Kodeli, E. Sartori, E. Ivanov,
27 O. Cabellos, Benchmarks for uncertainty analysis in modelling (uam) for
28 the design, operation and safety analysis of lwrsvolume i: Specification
29 and support data for neutronics cases (phase i), Tech. rep., Organisation
30 for Economic Co-Operation and Development (2013).

31
32 [36] D. W. Nigg, D. A. Steuhm, Advanced test reactor core modeling update
33 project annual report for fiscal year 2011, Tech. rep., Idaho National Lab-
34 oratory (INL) (2011).

35
36 [37] Z. Sui, L. Cao, C. Wan, X. Zou, Covariance-oriented sample transformation:
37 A new sampling method for reactor-physics uncertainty analysis, Annals of
38 Nuclear Energy 134 (2019) 452–463.

39
40
41
42
43
44
45
46
47
48
49
50
51
52
53
54
55
56
57
58
59
60
61
62
63
64
65
7. Funding

The authors wish to acknowledge that this work was performed by funding
from Idaho National Laboratory (INL) by Battelle Energy Alliance, LLC under
contract DE-AC07-05ID14517.



Click here to access/download
Supplementary Interactive Plot Data (CSV)
bibs_used_in_thesisR0.bib